FURTHER NUMERICAL TESTS OF ENSEMBLE EDDY VISCOSITY METHODS

NAN JIANG AND WILLIAM LAYTON

Abstract. This supplementary material complements the report with similar title.

1. Introduction

The problem of computing ensembles, u_j, p_j, of solutions of the Navier-Stokes equations (**NSE**):

$$u_{j,t} + u_j \cdot \nabla u_j - \nu \triangle u_j + \nabla p_j = f_j(x,t), \text{ in } \Omega,\ j = 1, ..., J \tag{1.1}$$
$$\nabla \cdot u_j = 0, \text{ and } u_j(x,0) = u_j^0(x), \text{ in } \Omega \text{ and } u_j = 0, \text{ on } \partial\Omega.$$

was studied in a paper with similar title. This supplement presents further tests. The method uses two new ensemble eddy viscosity (**EEV**) type turbulence models with turbulent viscosity parametrizations

$$\textbf{EEV1:}\quad \nu_T = \mu_1 \triangle x |u'|, \quad \text{and}$$
$$\textbf{EEV2:}\quad \nu_T = \mu_2 |u'|^2 \triangle t.$$

These are based on direct parameterization of the energy in the turbulent fluctuations, $\frac{1}{2}|u'|^2$ and *a redefinition of the LES lengthscale* from (the usual) $l = \triangle x$ to

$$l = \textit{ distance a fluctuating eddy travels in one time step} = |u'| \triangle t.$$

1.1. **Methods.** The euclidean length of a vector and Frobenius norm of an array is $|\cdot|$. The symmetric part of the velocity gradient tensor is denoted ∇^s. The ensemble mean $< u >$**,** fluctuation u_j', its magnitude $|u'|$ and the induced kinetic energy density k' are

$$\text{mean: } < u > := \frac{1}{J} \sum_{j=1}^{J} u_j, \text{ fluctuation: } u_j' := u_j - < u > ,$$

$$|u'|^2 := \sum_{j=1}^{J} |u_j'|^2 \text{ and energy density: } \ k' = \frac{1}{2}\ |u'|^2(x,t).$$

Date: June 2013.

2000 *Mathematics Subject Classification.* Primary 65M12; Secondary 65J08 .

Key words and phrases. NSE, ensemble calculation, UQ.

The research herein was partially supported by NSF grant DMS 1216465 and Air Force grant FA 9550-12-1-0191.

Suppress the secondary spacial discretization and let superscripts denote the timestep number. Thus, for example, $< u >^n, u_j'^n$ denote respectively approximations to

$$\frac{1}{J}\sum_{j=1}^{J} u_j(\cdot,t_n) \text{ and } u_j(\cdot,t_n) - < u >^n, t_n := n\triangle t.$$

We have the method: for $j = 1, ..., J,\ \nabla \cdot u_j^{n+1} = 0,$ and

$$\begin{aligned} &\frac{u_j^{n+1}-u_j^n}{\Delta t} + < u >^n \cdot \nabla u_j^{n+1} + (u_j^n - < u >^n) \cdot \nabla u_j^n \\ &+\nabla p_j^{n+1} - \nu\Delta u_j^{n+1} - \nabla \cdot (\nu_T(l^n, k'^n)\nabla^s u_j^{n+1}) = f_j^{n+1}. \end{aligned} \tag{1.2}$$

The ensemble eddy viscosity parameterization is the coefficient $\nu_T(\cdot)$. Briefly, the Kolmogorov-Prandtl relation gives

$$\begin{aligned} \nu_T(\cdot) &= Const.l\sqrt{k'} \\ l = &\text{ mixing length of fluctuations,} \\ k' = &\text{ kinetic energy in fluctuations.} \end{aligned}$$

Often extensive (and optimistic) modelling steps are needed to generate representations of these two quantities, e.g., [34], [29]. Algorithm (1.2) allows direct calculation of both:

$$k' = \frac{1}{2}|u'|^2 \text{ and } l = \begin{cases} \text{either } \triangle x, \\ \text{or } |u'|\triangle t \end{cases}.$$

This gives

$$\begin{aligned} &\textbf{EEV1:} \quad \nu_T = \mu_1 \triangle x |u'|, \quad \text{and} \\ &\textbf{EEV2:} \quad \nu_T = \mu_2 |u'|^2 \triangle t. \end{aligned}$$

2. Supplementary Material: Further Numerical Tests of Ensemble Eddy Viscosity Methods

In our report, the following tests are presented.

Test 1 was for *flow between offset cylinders* driven by a rotating body force ($Re = 800$).

Test 2 compared EEV1 and EEV2 for the same geometry at $Re = 800, 1200, 2400$ and constant timestep $\triangle t = 0.025$.

Test 3 (results given in the supplementary materials) repeated these two tests but *reinitialized the perturbations* at $t = 1, 2, 3, \cdots$. The conclusions regarding stability were not altered by reinitialization.

Test 4 was an accuracy test with a smooth, known exact solution. In Test 4 *both EEV1 and EEV2 produced 2 significant digits of accuracy with* $\triangle x = 0.1$, an acceptable result.

Test 5 is a flow in a *channel with 2 outlets and a constriction* from [4, 18, 23]. Both EEV1 and EEV2 gave the correct general outlines of the flow (compared to others published results) and differences in the smaller details of the flow.

We performed further tests of EEV1 and EEV2 and variants that, while interesting, confirmed or were consistent with the preliminary results presented in our report. We present some of these explorations in this supplementary section.

Test 1: Stability of no EEV vs. EEV2 for flow between offset circles. Recall that the domain is

$$\Omega = \{(x, y) : x^2 + y^2 \leq r_1^2 \text{ and } (x - c_1)^2 + (y - c_2)^2 \geq r_2^2\}$$

a disk with a smaller, off-center obstacle inside with no-slip boundary conditions on both circles. Let $r_1 = 1$, $r_2 = 0.1$, $c = (c_1, c_2) = (\frac{1}{2}, 0)$. The flow is driven by:

$$f(x, y, t) = (-4y * (1 - x^2 - y^2), 4x * (1 - x^2 - y^2))^T.$$

The mesh has $n = 40$ mesh points around the outer circle and $m = 10$ mesh points around the immersed circle, and extended to Ω as a Delaunay mesh. We begin with $Re = 800$ and then increase Re.

Generation of the initial conditions. Perturbations of $u_j^0, j = 1, 2$, and u_0^0 (with $\epsilon \equiv 0$, 'no perturbation'), are generated by solving the steady Stokes problem on the same geometry with $\epsilon = 10^{-3}$ and

$$f_1(x, y, t) = f(x, y, t) + \epsilon * (sin(3\pi x)sin(3\pi y), cos(3\pi x)cos(3\pi y))^T,$$
$$f_2(x, y, t) = f(x, y, t) - \epsilon * (sin(3\pi x)sin(3\pi y), cos(3\pi x)cos(3\pi y))^T,$$

The Navier-Stokes equations are then solved with these initial conditions, giving u_1, u_2, $u_{ave} = (u_1 + u_2)/2$ and u_0 (initial condition u_0^0 -'no perturbation').

Quantities plotted. The report gave plots of volume averaged statistics. Here we supplement these with streamlines and contour plots of vorticity over $0 \leq t \leq 10$. The timestep is adapted as in the report. First we plot total energy dissipation rates of EEV2 and noEV and power input rates of both.

Next plotted is EEV2 and noEV velocity vectors at $\nu = 1/800$. Note that at this Reynolds number the flow already begins to have interesting features and that the noEV velocities begin to exhibit radial oscillations.

This pattern is confirmed by the contour plots of vorticity. The noEV vorticity contours reveal small scale oscillations clearly.

Next the Reynolds number was increased to $Re = 1200$ and 2400. We observed that EEV2 remained stable with $\triangle t = 0.05$ at both $Re = 1200$ and 2400. With NoEV, adapting the timestep ensured stability but forced a very small timestep and execution time so long that the method failed to reach the final time. The EEV2 solutions are given below.

Test 2: Stability of EEV1 vs. EEV2. Test 1 was repeated comparing EEV1 and EEV2 for $Re = 800$ and constant timestep. We take $\Delta t = 0.025, Re = 800, \mu_2 = 1, \mu_1 \Delta x = 0.2$. The streamlines very clearly show that by $t = 10.0$, the EEV1 approximation returns to the Stokes flow initial condition while EEV2 continues its evolution.

The over diffusion in EEV1 vs. EEV2 is also clear from the kinetic energy plot.

Test #3: Re-initialization: We repeat Test 2 but reinitialize the perturbation at $t = 1, 2, 3, \cdots$, restarting with initial data being the average produced up to that point and the same perturbations as at $t = 0$, as in Test #1. We use the same constant timestep $\Delta t = 0.025, Re = 800, \mu_2 = 1, \mu_1 \Delta x = 0.2$. The plots show that EEV1 results improved somewhat but still EEV1 over-diffuses while EEV2 does not.

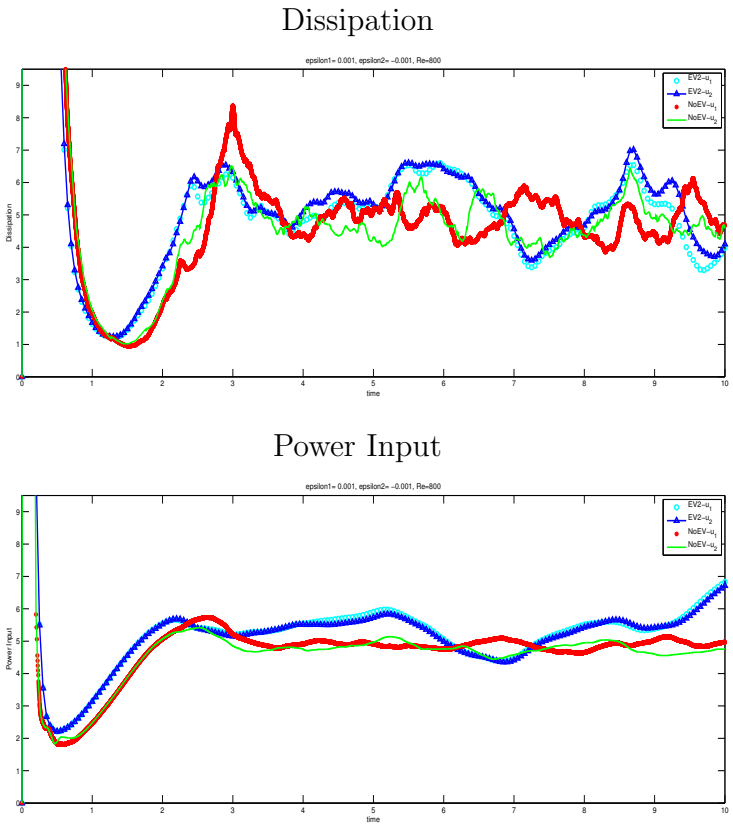

FIGURE 1. EV2 vs. NoEV: Dissipation & Power Input, $\nu = 1/800$

REFERENCES

[1] O. AXELSSON, *A survey of preconditioned iterative methods for linear systems of algebraic equations*, BIT, 25 (1985), 166-187.

[2] L.C. BERSELLI, *On the large eddy simulation of the Taylor-Green vortex*, J. Math. Fluid Mech., 7 (2005), S164-S191.

[3] L.C. BERSELLI, T. ILIESCU AND W. LAYTON, *Mathematics of Large Eddy Simulation of Turbulent Flows*, Springer, Berlin, 2006.

[4] A.L. BOWERS AND L.G. REBHOLZ, *Numerical study of a regularization model for incompressible flow with deconvolution-based adaptive nonlinear filtering*, CMAME, 258 (2013), 1-12.

[5] S. BRENNER AND R. SCOTT, *The Mathematical Theory of Finite Element Methods*, Springer, 3rd edition, 2008.

[6] M. CARNEY, P. CUNNINGHAM, J. DOWLING AND C. LEE, *Predicting Probability Distributions for Surf Height Using an Ensemble of Mixture Density Networks*, International Conference on Machine Learning, (2005).

[7] M. CASE, V. ERVIN, A. LINKE AND L. REBHOLZ, *A connection between Scott-Vogelius elements and grad-div stabilization*, SINUM 49(2011), 1461-1481.

[8] Y.T. FENG, D.R.J. OWEN AND D. PERIC, *A block conjugate gradient method applied to linear systems with multiple right hand sides*, CMAME 127 (1995), 203-215.

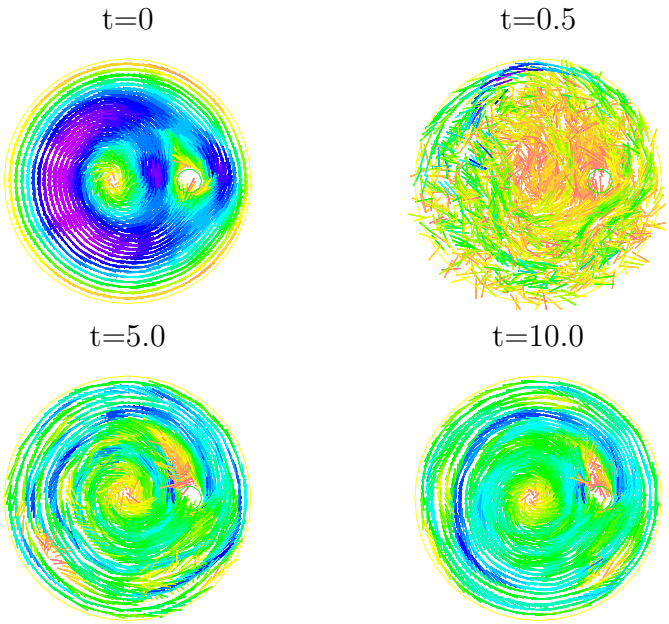

FIGURE 2. EV2: Velocity, $\nu = 1/800$

[9] P.F. FISCHER, *Projection techniques for iterative solution of Ax=b with successive right-hand sides*, CMAME, 163, 1998, 193-204.
[10] R.W. FREUND AND M. MALHOTRA, *A block QMR algorithm for non-Hermitian linear systems with multiple right-hand sides*, Linear Algebra and its Applications, 254, 1997, 119-157.
[11] E. GALLOPULOS AND V. SIMONCINI, *Convergence of BLOCK GMRES and matrix polynomials*, Lin. Alg. Appl., 247 (1996), 97-119.
[12] J.D. GIRALDO AND S.G. GARCÍA GALIANO, *Building hazard maps of extreme daily rainy events from PDF ensemble, via REA method, on Senegal River Basin*, Hydrology and Earth System Sciences, 15 (2011), 3605-3615.
[13] M.D. GUNZBURGER, *Finite Element Methods for Viscous Incompressible Flows - A Guide to Theory, Practices, and Algorithms*, Academic Press, (1989).
[14] A.E. GREEN AND G.I. TAYLOR, *Mechanism of the production of small eddies from larger ones*, Proc. Royal Soc. A., 158 (1937), 499-521.
[15] J.L. GUERMOND AND L. QUARTAPELLE, *On stability and convergence of projection methods based on pressure Poisson equation*, IJNMF, 26 (1998), 1039-1053.
[16] T.M. HAMILL, J.S. WHITAKER, M. FIORINO, S.E. KOCH AND S.J. LORD, *Increasing NOAA's computational capacity to improve global forecast modeling*, NOAA White Paper, 19 July 2010.
[17] F. HECHT AND O. PIRONNEAU, *FreeFEM++*, http://www.freefem.org.
[18] J. HEYWOOD, R. RANNACHER AND S. TUREK, *Artificial boundaries and flux and pressure conditions for the incompressible Navier-Stokes equations*, IJNMF, 22 (1996), 325-352.
[19] T.J.R. HUGHES, A.A. OBERAI AND L. MAZZEI, *Large eddy simulation of turbulent channel flows by the variational multiscale method*, Phys. Fluids., 13 (2001), 1784-1799.
[20] T. ILIESCU AND W. LAYTON, *Approximating the Larger Eddies in Fluid Motion III: the Boussinesq Model for Turbulent Fluctuations*, An. St. Univ. "Al. I. Cuza", vol. 44, (1998), 245-261.

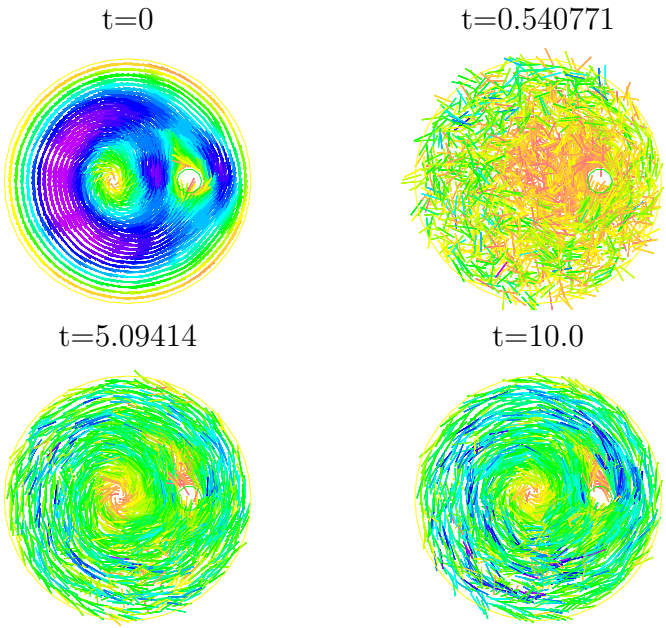

FIGURE 3. NoEV: Velocity, $\nu = 1/800$

[21] N. JIANG AND W. LAYTON, *An algorithm for fast calculation of flow ensembles*, submitted, April 2013, available at: http://www.mathematics.pitt.edu/sites/default/files/research-pdfs/ensemble2April2013.pdf.
[22] V. JOHN, *Large Eddy Simulation of Turbulent Incompressible Flows. Analytical and Numerical Results for a Class of LES Models*, Lecture Notes in Computational Science and Engineering 34, Springer-Verlag, Berlin, 2004
[23] P. KUBERRY, A. LARIOS, L. REBHOLZ AND N. WILSON, *Numerical approximation of the Voigt regularization for incompressible Navier-Stokes and magnetohydrodynamic flows*, Comput. Math. Appl., 64 (8) (2012), 2647-2662.
[24] W. LAYTON AND R. LEWANDOWSKI, *Analysis of an eddy viscosity model for large eddy simulation of turbulent flows*, J. Math. Fluid Mechanics, 2 (2002), 374-399.
[25] O.P. LE MAITRE AND O.M. KINO, *Spectral methods for uncertainty quantification*, Springer, Berlin, 2010.
[26] O.P. LE MAITRE, O.M. KINO, H. NAJM AND R. GHANEM, *A stochastic projection method for fluid flow, I. Basic Formulation*, JCP, 173 (2001), 481-511.
[27] W. LAYTON AND L. TOBISKA, *A Two-Level Method with Backtracking for the Navier–Stokes Equations*, SINUM, 35 (1998), pp. 2035-2054.
[28] M. LEUTBECHER AND T.N. PALMER, *Ensemble forecasting*, JCP, 227 (2008), 3515-3539.
[29] R. LEWANDOWSKI, *The mathematical analysis of the coupling of a turbulent kinetic energy equation to the Navier-Stokes equation with an eddy viscosity*, Nonlinear Analysis, 28 (1997), 393-417.
[30] J.M. LEWIS, *Roots of ensemble forecasting*, Monthly Weather Rev., 133 (2005), 1865-1885.
[31] W.J. MARTIN AND M. XUE, *Initial condition sensitivity analysis of a mesoscale forecast using very-large ensembles*, Mon. Wea. Rev., 134 (2006), 192-207.
[32] D.P. O'LEARY, *The block conjugate gradient algorithm and related methods*, Linear Algebra and its Applications, 29 (1980), 293–322,
[33] M. OLSHANSKII AND A. REUSKEN, *Grad-Div stabilization for the Stokes equations,* Math. of Comp. 73 (2004) 1699-1718.

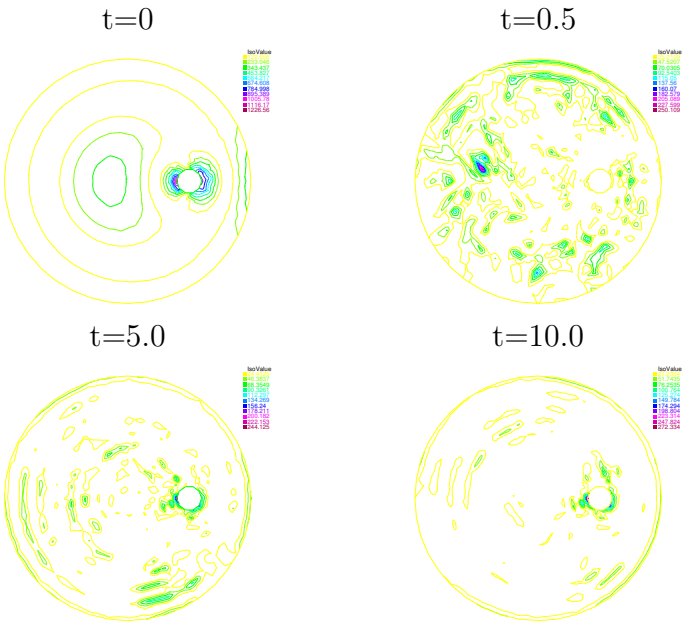

FIGURE 4. EV2: Contours of Vorticity, $\nu = 1/800$

[34] P. SAGAUT, *Large eddy simulation for Incompressible flows*, Springer, Berlin, 2001.
[35] D.J. STENSRUD, *Parameterization schemes: Keys to numerical weather prediction models*, Cambridge U. Press, 2009.
[36] G.I. TAYLOR, *On decay of vortices in a viscous fluid*, Phil. Mag., 46 (1923), 671-674.
[37] Z. TOTH AND E. KALNEY, *Ensemble forecasting at NMC: The generation of perturbations*, Bull. Amer. Meteor. Soc., 74 (1993), 2317-2330.

(All authors) DEPT. OF MATHEMATICS, UNIV. OF PITTSBURGH, PITTSBURGH, PA 15260, USA
E-mail address: naj24@pitt.edu, wjl@pitt.edu
URL: www.math.pitt.edu/~wjl

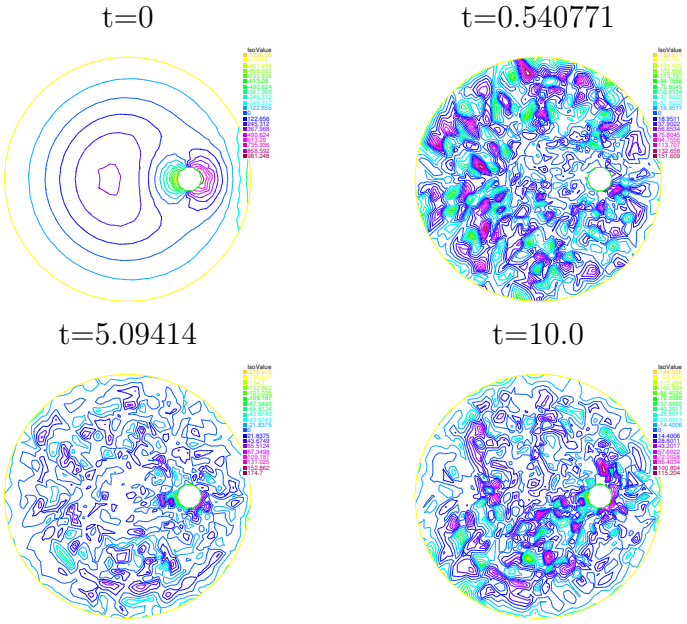

FIGURE 5. NoEV: Contours of Vorticity, $\nu = 1/800$

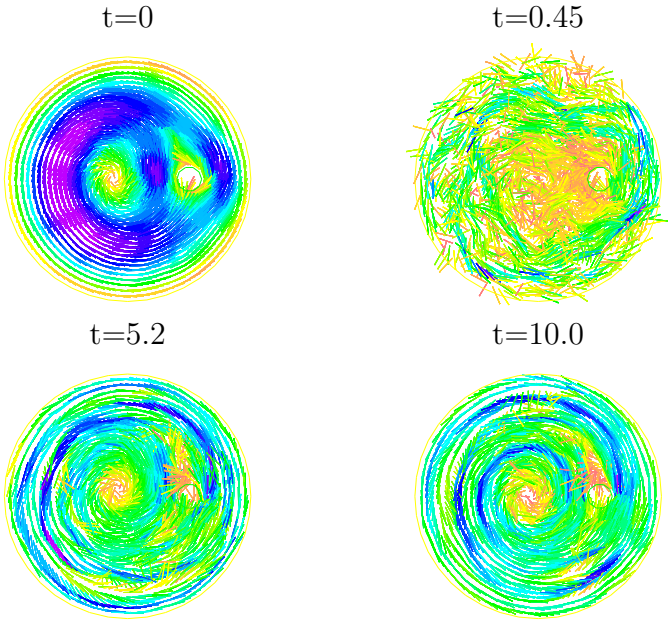

FIGURE 6. EEV2: Velocity, $\nu = 1/1200$

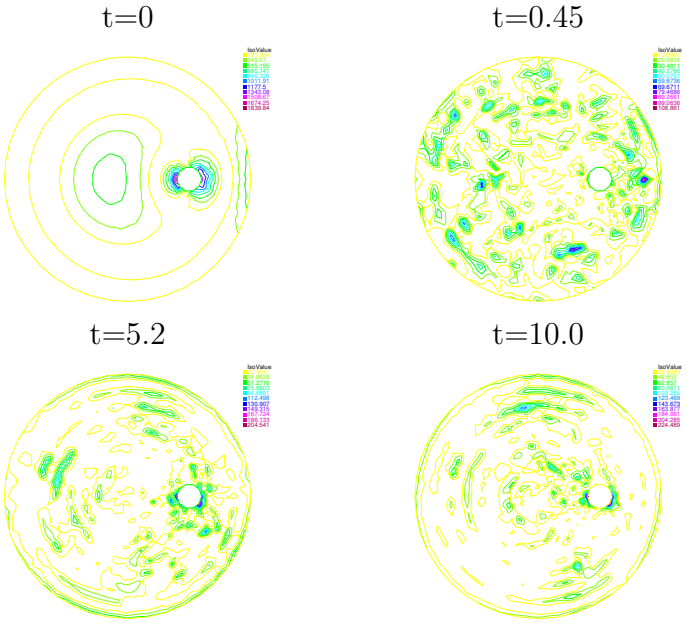

FIGURE 7. EEV2: Contours of Vorticity, $\nu = 1/1200$

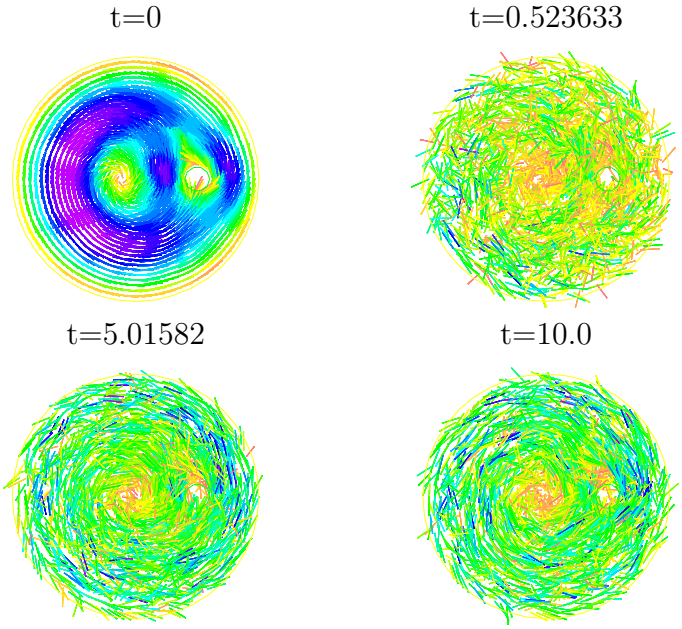

FIGURE 8. EEV2: Velocity, $\nu = 1/2400$

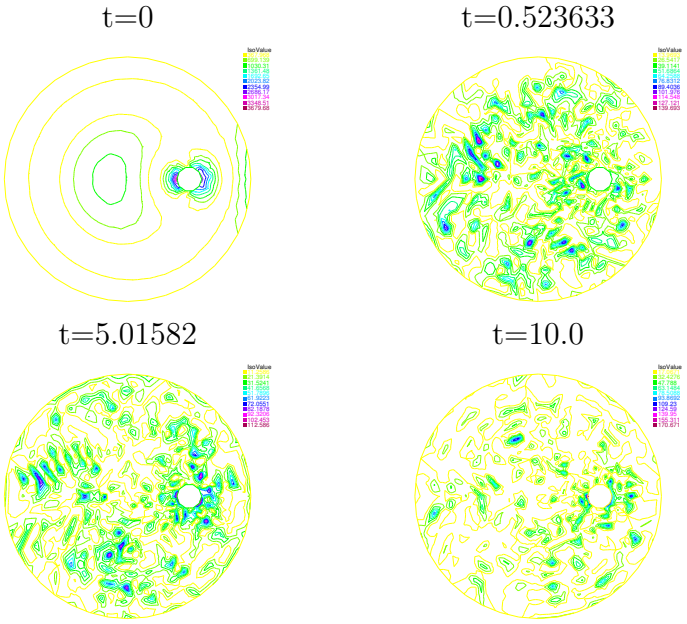

FIGURE 9. EEV2: Contours of Vorticity, $\nu = 1/2400$

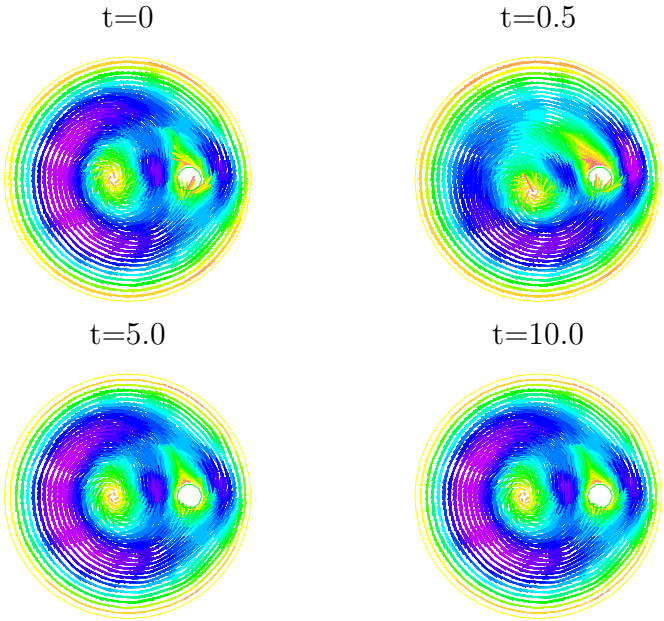

FIGURE 10. EV1 gives Stokes flow: Velocity, $\nu = 1/800$

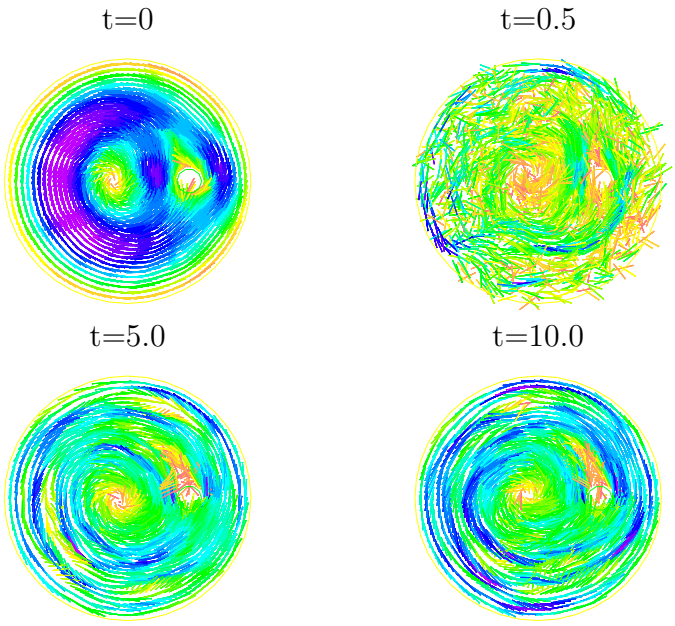

FIGURE 11. EV2: Velocity, $\nu = 1/800$

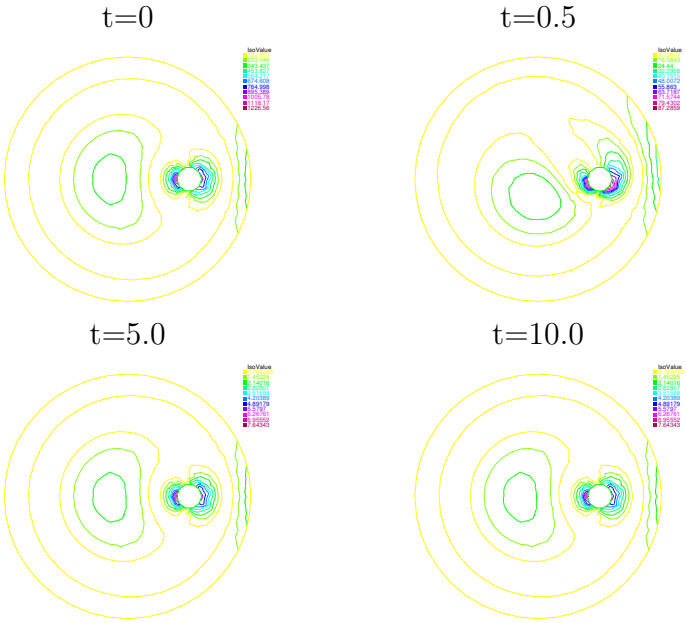

FIGURE 12. EV1 gives Stokes flow: Contours of Vorticity, $\nu = 1/800$

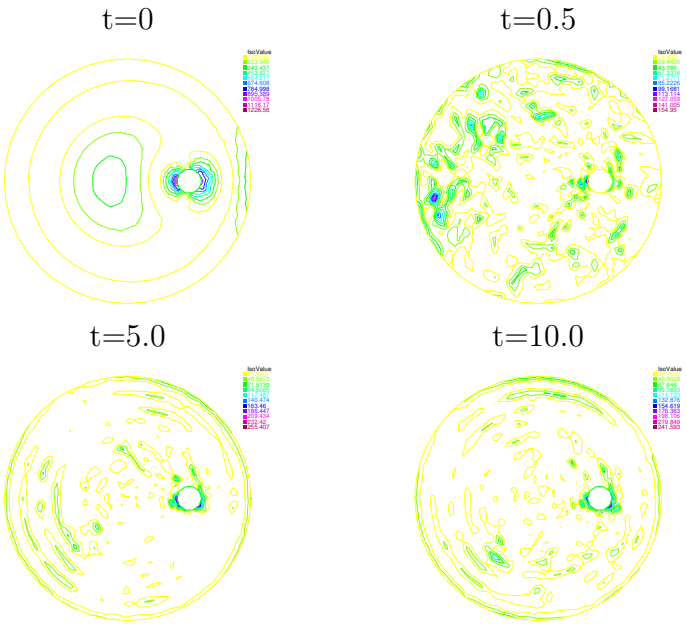

FIGURE 13. EV2: Contours of Vorticity, $\nu = 1/800$

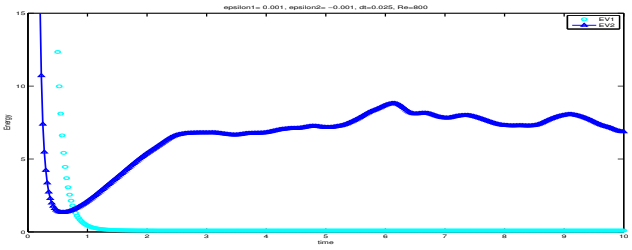

FIGURE 14. Energy: EV1 Vs EV2, $\Delta t = 0.025$, $\nu = 1/800$

EV1

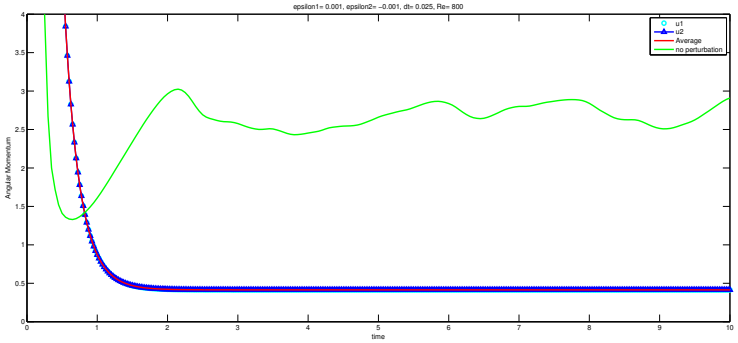

EV2

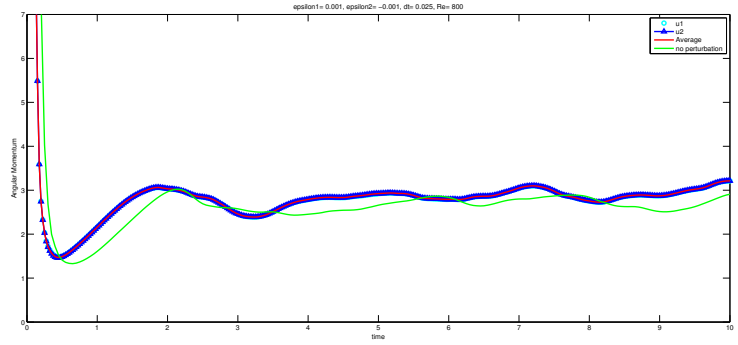

FIGURE 15. Reinitialize: Angular Momentum, $\nu = 1/800$

EV1

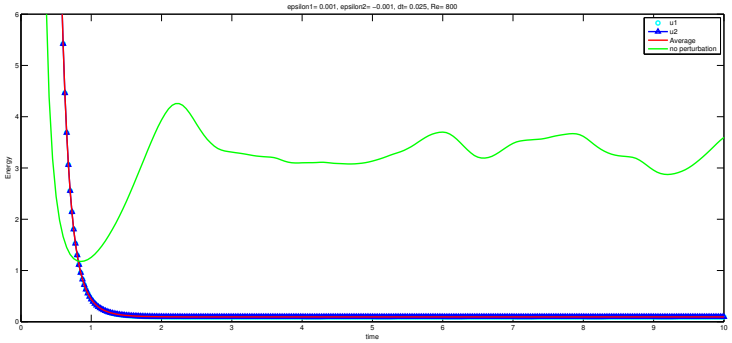

EV2

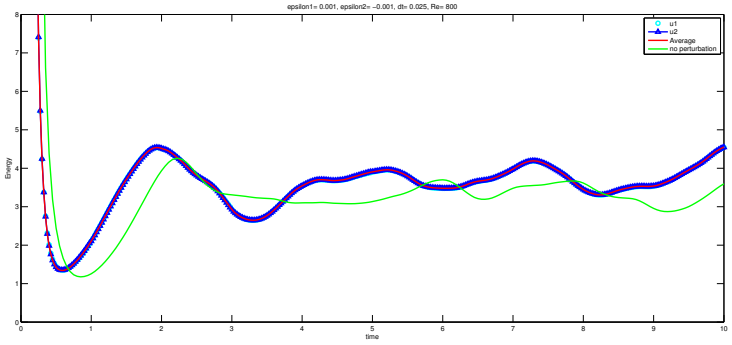

FIGURE 16. Reinitialize: Energy, $\nu = 1/800$

EV1

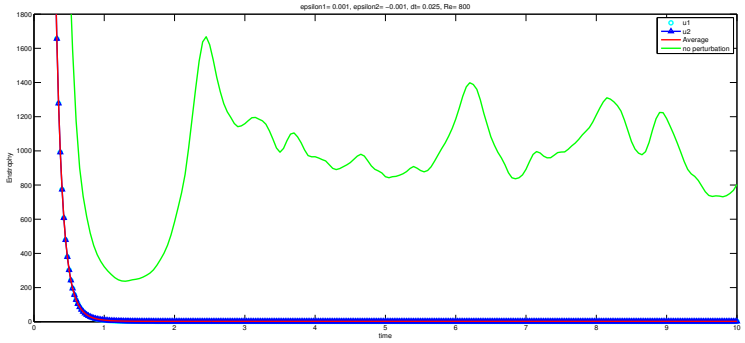

EV2

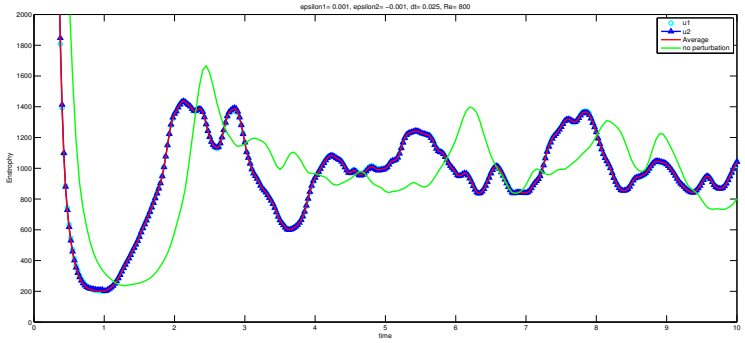

FIGURE 17. Reinitialize: Enstrophy, $\nu = 1/800$

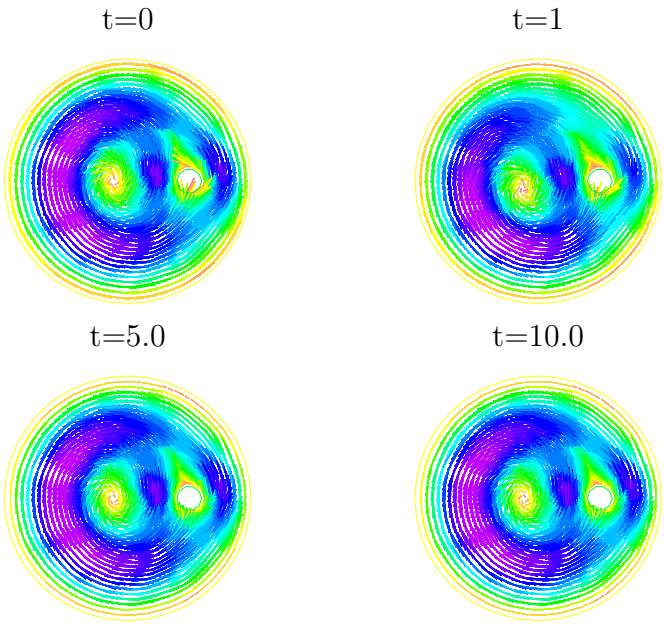

FIGURE 18. Reinitialize EV1: Stokes flow velocity, $\nu = 1/800$

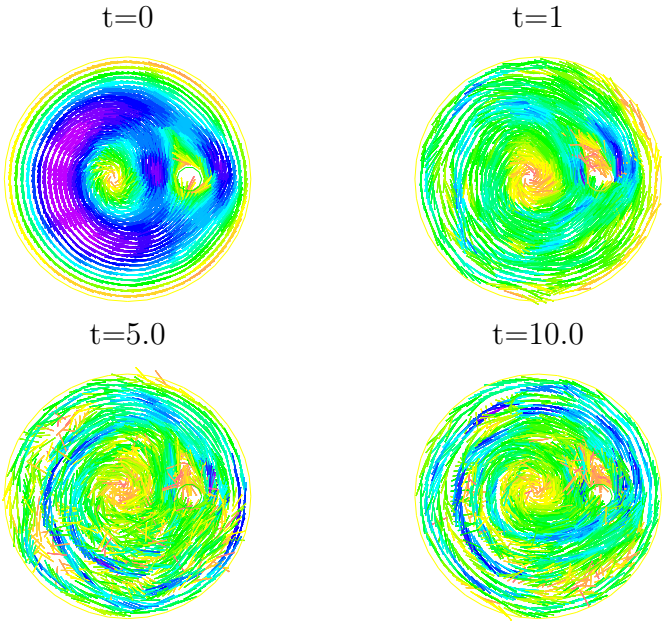

FIGURE 19. Reinitialize: EV2: Velocity, $\nu = 1/800$

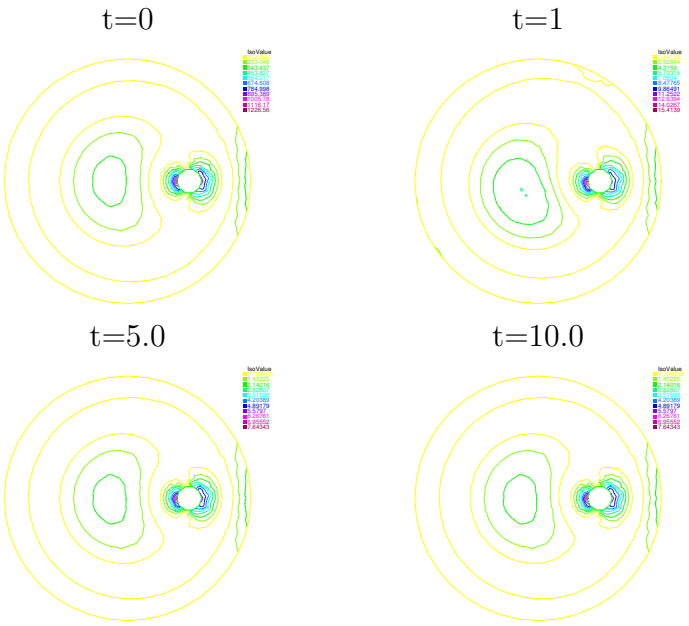

FIGURE 20. Reinitialize: EV1: Contours of Vorticity, $\nu = 1/800$

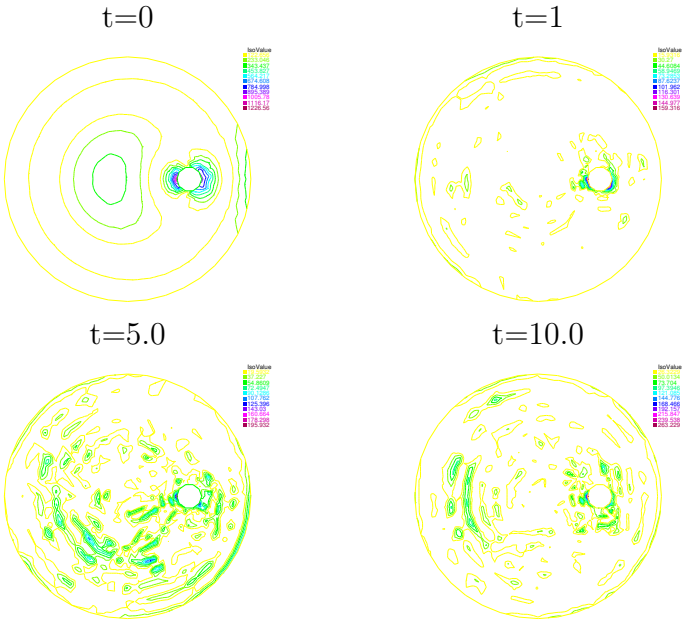

FIGURE 21. Reinitialize: EV2: Contours of Vorticity, $\nu = 1/800$

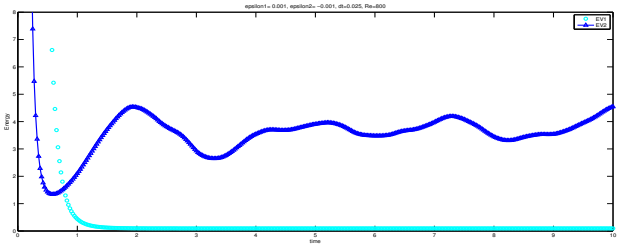

FIGURE 22. Reinitialize: Energy: EV1 Vs EV2, $\Delta t = 0.025$, $\nu = 1/800$